Acta Cryst. (1974). B30, 1278

Packing of Paraffin Chains in the Four Stable Modifications of n-Tritriacontane

BY W. PIESCZEK, G. R. STROBL AND K. MALZAHN

Institut für Physikalische Chemie der Universität Mainz, 65 Mainz, Jakob-Welder-Weg 15, Germany (BRD)

(*Received* 13 *December* 1973; *accepted* 22 *January* 1974)

The n-alkane $C_{33}H_{68}$ exhibits three phase transitions between room temperature and the melting point $T_m = 71{\cdot}8\,^{\circ}C$. The modes of chain packing in the four modifications (A, B, C, D) were determined from Weissenberg photographs. Modification A, existing at temperatures $< 54{\cdot}5\,^{\circ}C$, is the known orthorhombic form (space group *Pcam*) generally found at low temperatures for odd-numbered paraffins. The modifications B and C, which are stable in the temperature ranges $54{\cdot}5\,^{\circ}C < T < 65{\cdot}5\,^{\circ}C$ and $65{\cdot}5\,^{\circ}C < T < 68\,^{\circ}C$, possess monoclinic unit cells (with space groups Aa and $A2$ respectively), the crystals being twins. In the high-temperature form D, the so-called 'rotator-phase', the crystalline order is strongly disturbed. Only a few low-order reflexions exist. Their positions in reciprocal space show that the chain axis is tilted from the normal to the end group planes by approximately 19·5°. The lateral packing closely approaches a hexagonal form but does not reach it.

Introduction

Crystalline paraffins are known to exist in different polymorphic forms (Broadhurst, 1962). The different modifications depend on the number of methylene units and the temperature. At low temperatures, three different modifications are found: an orthorhombic one if the number of carbon atoms n is odd, and if n is even a triclinic or monoclinic one depending on whether $n < 26$ or $n > 26$ respectively. X-ray structure determinations have been carried out for these modifications (Smith, 1953; Müller & Lonsdale, 1948; Shearer & Vand, 1956).

Paraffins with carbon numbers $9 \le n_{odd} \le 39$ or $20 \le n_{even} \le 38$ show a phase transition several degrees below the melting point. The high-temperature form is usually called the 'rotator-phase', expressing the commonly held view that the chains rotate quasi-freely about their axes (Müller, 1932; Hoffmann, 1952; McClure, 1968). Calorimetric measurements suggest that the structure of this modification is different for different ranges of chain length; plots of the heats of transition and fusion *versus* the chain length are essentially linear for $n > 26$, and $n < 20$, but show anomalies in the intermediate range. An X-ray analysis of $C_{19}H_{40}$ shows that the lateral arrangement of the chains has hexagonal symmetry, as required for rotating molecules (Larsson, 1967). Results on longer chains have not been reported.

Generally the solid-phase behaviour is very sensitive to the purity. Recently Heitz and Peters synthesized pure $C_{33}H_{68}$ by a method similar to that described (Heitz, Wirth, Peters, Strobl & Fischer, 1972). $C_{33}H_{68}$ exhibits three phase transitions before melting. Fig. 1 gives the observed thermogram. We choose the letters A, B, C and D to denote the four solid phases occurring with increasing temperature. A is the known orthorhombic modification, D corresponds to the 'rotator-phase'; the modifications B and C have not been reported on before.

X-ray scattering experiments were used to determine the structures of these four modifications. Difficulties arose from the poor quality and the complex character of the Weissenberg photographs. One reason for this is that on reaching modification C the plane surface on the thin, lozenge-shaped crystals is destroyed and twinning occurs. In spite of these complications it was possible to derive information about the chain packing from the positions of some specially strong reflexions. The reason is that in principle only a few parameters can be varied when paraffin chains are packed in a crystal. The values of these packing parameters could be determined with sufficient accuracy.

We have also investigated the birefringence of the crystals in a polarizing microscope. These simple measurements can be used for determining the orientations of the zigzag planes of the molecules. X-ray measurements yield only rough values for this 'setting angle'.

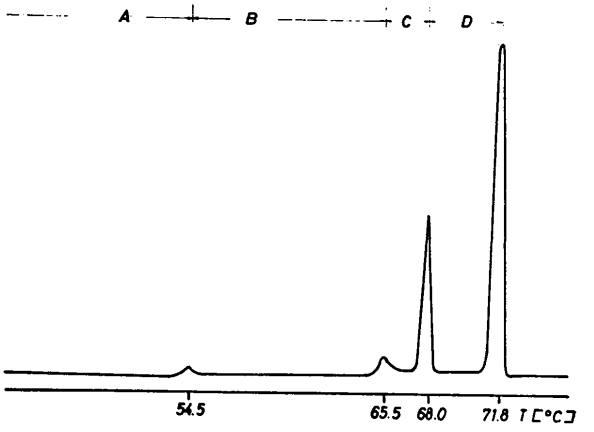

Fig. 1. $C_{33}H_{68}$, crystallized from solution, DSC-thermogram showing four solid modifications A, B, C, D. Transitions occur at the temperatures $T_{AB} = 54{\cdot}5$, $T_{BC} = 65{\cdot}5$ and $T_{CD} = 68\,^{\circ}C$ with heats of transition $\Delta H_{AB} = 0{\cdot}5$, $\Delta H_{BC} = 1{\cdot}1$ and $\Delta H_{CD} = 7{\cdot}0$ kcal mol^{-1}. The heat of fusion is $\Delta H_f = 19{\cdot}0$ kcal mol^{-1}.

Packing properties of crystalline paraffins

Crystals of paraffin molecules have a lamellar structure. They are composed of stacked layers, each layer consisting of chain molecules lying with their axes parallel to each other. The end groups are situated in the lamellar surfaces. This general building scheme has been studied extensively by Kitaigorodskii (1961) and by Segerman (1965). Packing considerations led to the conclusion that all possible structures can be classified by specifying a few packing parameters. The first group of parameters describes the lateral packing of the C_2H_4 units, which are arranged in 'subcells'. Two types have been found. For the majority the subcell is orthorhombic and occupied by two C_2H_4 groups. The other type, a triclinic subcell containing one C_2H_4 group, is found only for the triclinic modification of even-numbered paraffins. The second group of parameters

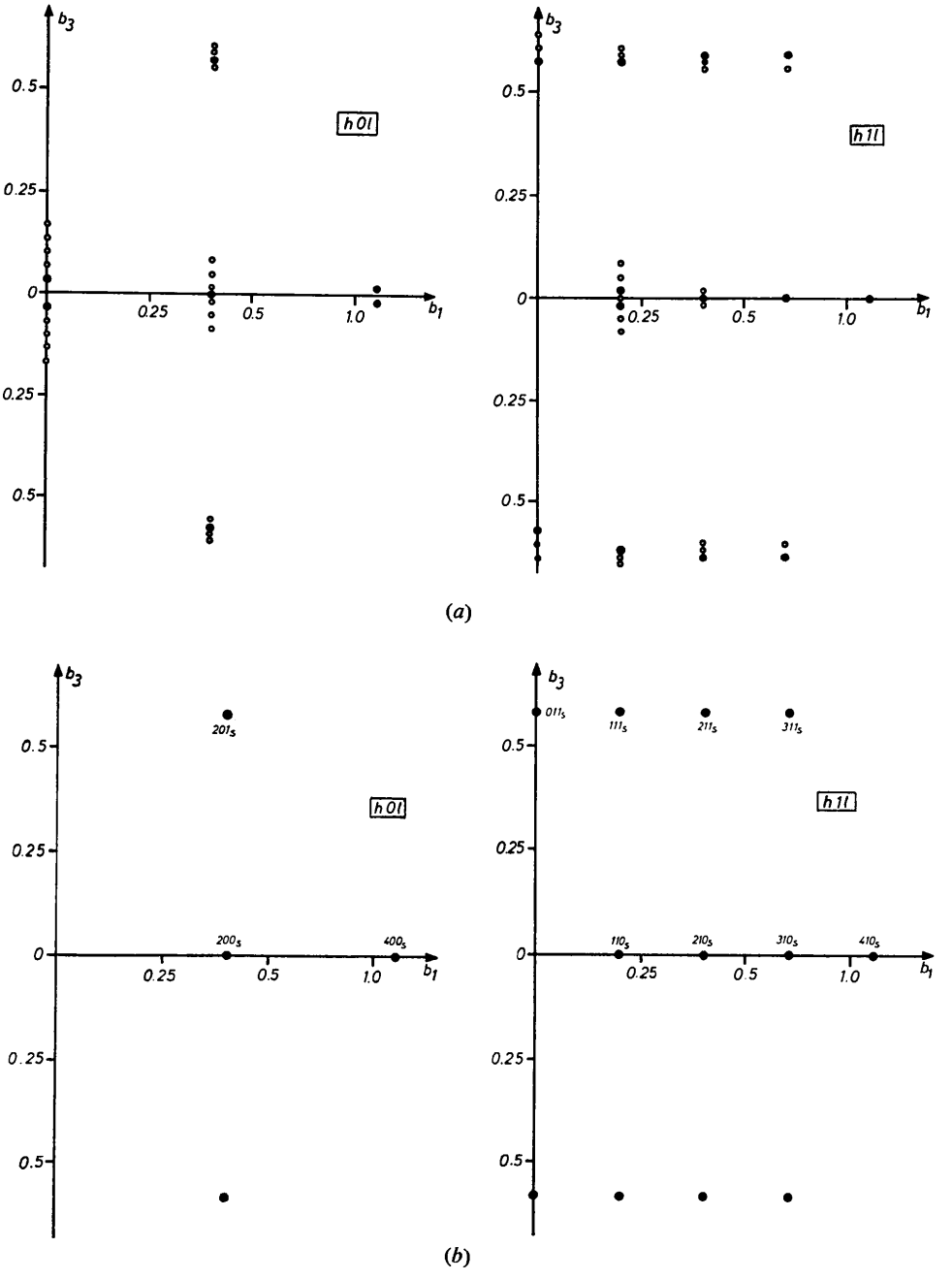

Fig. 2. Modification *A*. (*a*) Observed reflexion groups in the reciprocal lattice planes *h*0*l*, *h*1*l*. Filled circles indicate the strongest reflexions for each group. (*b*) Positions of corresponding sublattice reflexions *h*0l_s and *h*1l_s.

determines the type of the layer surface. It can be perpendicular to the chain direction ('rectangular layer') or inclined ('oblique layer'). This surface has to be a lattice plane with reference to the subcells and may be indexed as $(hkl)_s$ (here and in the following an s indicates the subcell lattice). The third group of parameters characterizes the layer stacking. Neighbouring lamellae are related by a shift Δ_{ch} in chain direction which is eventually accompanied by a 180° turn about the chain axis, and subsequent shifts Δ_a and Δ_b parallel to the lamellar surface.

These three groups of packing parameters influence the scattering behaviour in different ways. In principle a paraffin crystal can be regarded as a one-dimensional array of layer-like particles. Hence, the scattered intensity may be written as a product

$$J(b) \sim |F_L|^2(b) \,.\, G(b)$$

of the structure factor of the single layers and a lattice factor $G(b)$, which depends solely on the mode of stacking (b denotes the reciprocal-lattice vector). The 'particle factor' $|F_L|^2(b)$ shows maxima at the reflexion positions hkl_s or, in other words, at the reflexion points of a hypothetical extended-chain polyethylene crystal with the same lateral packing as in the paraffin layer. Due to the finite thickness of the layers, these subcell reflexions are elongated in a direction perpendicular to the layer surface. Hence, the particle factor $|F_L|^2$ differs from zero only along finite 'rods' localized at the reflexion points of a corresponding polyethylene crystal. If now the layers are regularly stacked, the lattice factor $G(b)$ picks out a series of discrete reflexion points along these rods. Thus, in the case of a paraffin crystal, groups of reflexions are observed with their centres at the positions of the reflexions hkl_s of the equivalent polyethylene crystal. Thus each group represents a 'split' sublattice reflexion hkl_s. In addition, a series of reflexions is found in the small-angle region. These $00l$ reflexions demonstrate the lamellar structure of a paraffin crystal directly.

Fig. 2 shows the reflexion distribution in reciprocal space found for modification A. The plot is limited to the scattering range $\theta < 30°$. For comparison the positions of the subcell reflexions are given. They correspond to an orthorhombic subcell with dimensions $a_s = 7{\cdot}44$, $b_s = 4{\cdot}96$, $c_s = 2{\cdot}54$ Å.

X-ray scattering experiments

Crystals obtained from dilute petroleum spirit solution were plate-like and lozenge-shaped. Oscillation and Weissenberg photographs were obtained from crystals rotating around the short diagonal. This turned out to be a common crystallographic direction for all four modifications. Fig. 3 shows a typical crystal with the reference coordinate system x_1, x_2, x_3. The related reciprocal-space coordinates are b_1, b_2, b_3. Crystals were heated in a furnace with a window which permitted the registration of all reflexions with $\theta < 30°$. In order to prevent bending of the thin crystals they were put on a glass micro-slide. In addition to the Weissenberg photographs on individual crystals, powder diagrams were recorded with a diffractometer for a more precise determination of reflexion angles. The experiments were performed with Cu $K\alpha$ radiation, $\lambda = 1{\cdot}542$ Å.

Birefringence measurements for determining the setting angle

A complete description of the lateral packing of the methylene groups requires in addition to the subcell constants a knowledge of the orientation of the zigzag planes of the molecules. This orientation is usually specified by giving the angle between their planes and the $(100)_s$ plane. For the orthorhombic subcell this 'setting angle' is roughly $\varphi \simeq 45°$. A more precise determination by X-ray scattering experiments is difficult, since the correct anisotropic temperature factors are unknown. A simple way of estimating it is provided by birefringence measurements. The three axes of the optical indicatrix are parallel to $\mathbf{a}_s, \mathbf{b}_s, \mathbf{c}_s$. The refractive index in the chain direction is $n_c = 1{\cdot}588$ (Hartshorne & Stuart, 1970); the average value perpendicular to it is $(n_a + n_b)/2 = 1{\cdot}521$. The separate values n_a, n_b follow by measuring the directions of the optic axes. At 25°C these were found to lie in the $(010)_s$ plane, enclosing angles of $\pm 14{\cdot}2 \pm 0{\cdot}1°$ with the chain direction $\mathbf{c}_s$. This leads to $n_a = 1{\cdot}523$, $n_b = 1{\cdot}519$.

On the other hand, n_a and n_b can be calculated from the known bond polarizabilities (Hartshorne & Stuart, 1970)

$$\alpha_{\parallel}^{CC} = 0{\cdot}97 \times 10^{-24}, \quad \alpha_{\perp}^{CC} = 0{\cdot}25 \times 10^{-24},$$
$$\alpha_{\parallel}^{CH} = 0{\cdot}82 \times 10^{-24}, \quad \alpha_{\perp}^{CH} = 0{\cdot}6 \times 10^{-24} \text{ cm}^{-3}$$

by use of the Lorentz–Lorenz equation:

$$\frac{n_{a,b}^2 - 1}{n_{a,b}^2 + 2} \cdot \frac{M}{\varrho} = \frac{4\pi}{3} \cdot L\alpha_{a,b}$$

with

$$\alpha_{a,b} = \sum_i \alpha_i \,.\, \cos^2 \delta_{a,b}^i + \alpha_{\perp}^i \,.\, \sin^2 \delta_{a,b}^i \,.$$

M is the molecular weight of the two methylene units in the subcell, ϱ is the density in the subcell lattice, and L is Avogadro's number. $\delta_{a,b}^i$ is the angle between the bond i and the edges a_s and b_s respectively.

After introduction of the known bond angles relative to the zigzag plane this equation yields the refractive indices and thus their difference $\Delta n = n_b - n_a$ as a function of the setting angle φ (Fig. 4). By comparison with the experimental value for Δn the setting angle can be determined. Due to uncertainties in the bond polarizabilities this is only an estimate, but one conclusion is valid: $n_b > n_a$ means $\varphi < 45°$, $n_b < n_a$ means $\varphi > 45°$. In addition, the direction of change with changing temperature can be judged.

Measurements of Δn were performed with a Berek

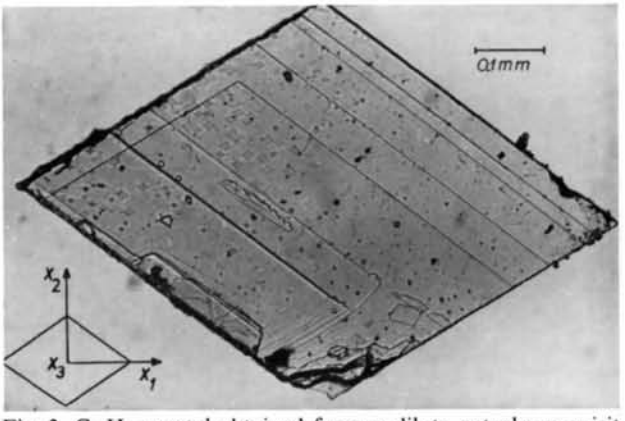

Fig. 3. $C_{33}H_{68}$ crystal obtained from a dilute petroleum spirit solution. Definition of a reference coordinate system x_1, x_2, x_3

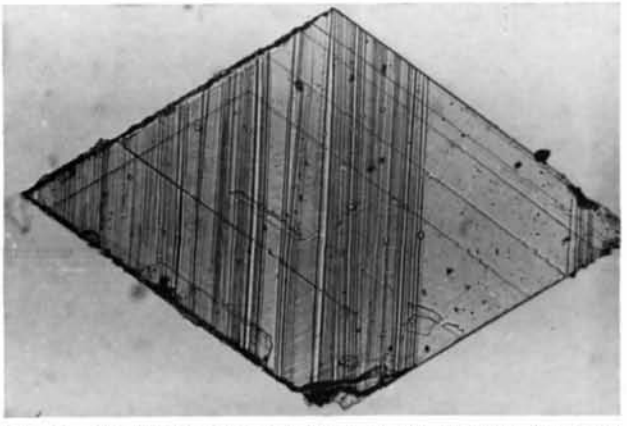

Fig. 11. Modification *C*. Structure of the lamellar interface.

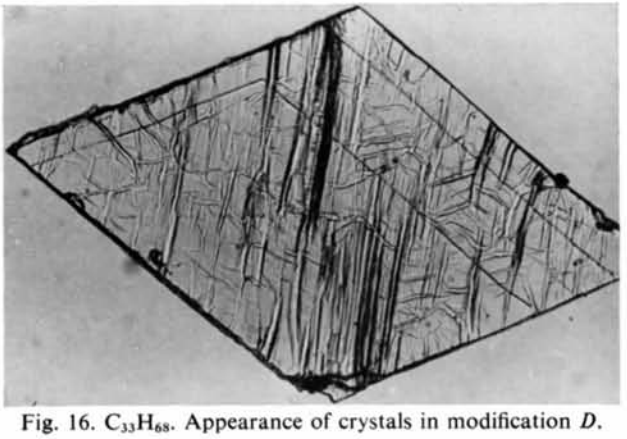

Fig. 16. $C_{33}H_{68}$. Appearance of crystals in modification *D*.

To face p. 1280

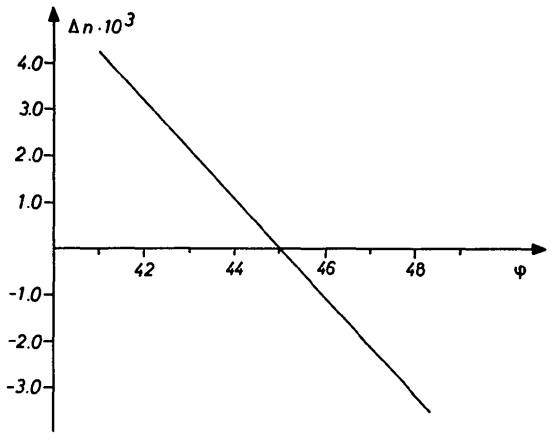

Fig. 4. Relation between the birefringence $\Delta n = n_b - n_a$ and the setting angle φ of the zigzag plane calculated for an orthorhombic subcell ($a_s = 7{\cdot}44$, $b_s = 4{\cdot}96$, $c_s = 2{\cdot}54$ Å) from the Lorentz–Lorenz equation.

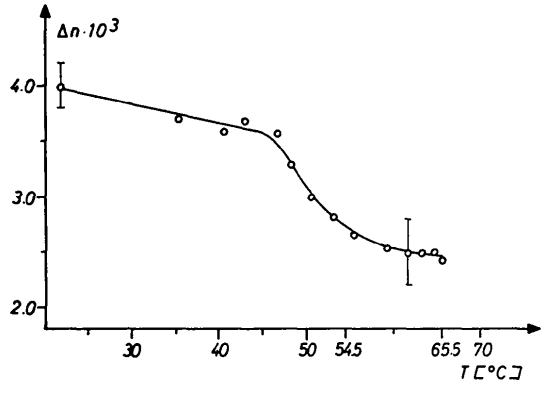

Fig. 5. Birefringence Δn as a function of the temperature T for the modifications A and B.

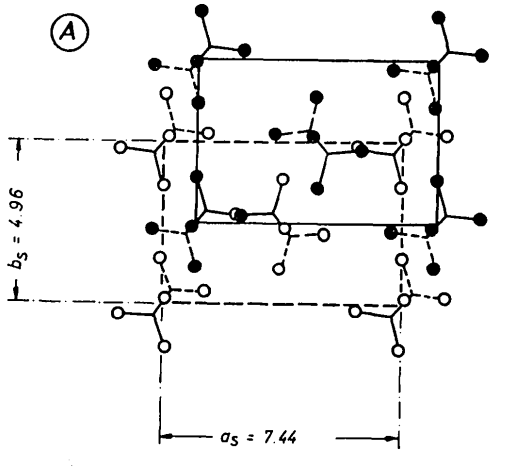

Fig. 6. Modification A. Projection along the chain axis.

compensator. The birefringence Δn was determined as a function of temperature through the ranges of the modifications A and B (Fig. 5).

Evalution of the scattering diagrams of the high temperature forms

All essential properties of the mode of chain-packing in a paraffin crystal are reflected directly in the appearance of scattering diagrams and can be derived from the positions of a limited number of reflexions.

For any paraffin crystal six characteristic reflexion groups with outstanding intensities exist. If the subcell is orthorhombic they represent the 'split' sublattice reflexions 200_s, $\bar{2}00_s$, 110_s, $\bar{1}\bar{1}0_s$ $\bar{1}10_s$, $1\bar{1}0_s$; for a triclinic sublattice they correspond to the reflexions 100_s, $\bar{1}00_s$, 010_s, $0\bar{1}0_s$, $\bar{1}10_s$, $1\bar{1}0_s$. The centres of these reflexion groups are coplanar in reciprocal space and determine the chain direction as being perpendicular to the common plane. Their positions yield the lateral subcell edges.

Within each group the reflexions are distributed along a straight line. This line is oriented perpendicular to the end-group planes and thus indicates their orientation relative to the sublattice.

The distance between adjacent reflexions in a group is related to the layer thickness L. A more detailed inspection of the reflexion positions can yield the stacking parameters $\Delta_a, \Delta_b, \Delta_{ch}$.

We see that all packing parameters can be derived from zero and first-level Weissenberg photographs. With a knowledge of the packing parameters we can give a crystallographic description of the lattice.

This method is generally applicable for chain molecular crystals with lamellar structure. If intensities are available the derived structure can serve as a starting model for refinement.

In our case two facts spoke against a refinement. To maintain a uniform crystal orientation through the different modifications proved to be very difficult. Although the disorientation never became too great, it prevented accurate measurement of intensities. The second complication is more serious. We know from other experiments (Strobl, Ewen, Fischer & Piesczek, 1974) that various kinds of lattice defects (rotations of chains about their axes in subsidiary minima, shifts along their axes, intra-chain defects) occur in the high-temperature modifications. For any detailed evaluation of intensities these defects have to be taken into account, which precludes a straightforward application of conventional refinement procedures.

Chain packing in the four modifications

1. *Modification A* ($T < 54{\cdot}5$°C)

Inspection of the scattering diagrams confirmed the structure reported by Smith (1953), with slightly different lattice constants. The lattice is orthorhombic, space group *Pcam* (conditions limiting reflexions are

$h0l$: $h=2n$; $0kl$: $l=2n$). The unit cell contains four molecules and has

$$a = 7{\cdot}44 \pm 0{\cdot}005 \text{ Å}$$
$$b = 4{\cdot}96 \pm 0{\cdot}005$$
$$c = 87{\cdot}65 \pm 0{\cdot}02 .$$

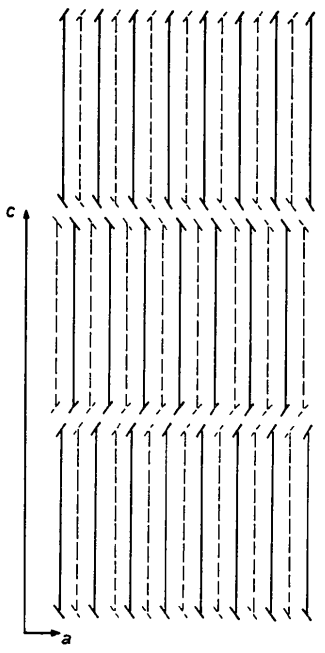

Fig. 7. Modification *A*. Schematic drawing of the chain packing viewed along **b**.

Approximate intensities of 90 reflexions were obtained by visual estimation from Weissenberg photographs and additionally by measuring the peak areas of powder diagrams (corrected for Lorentz–polarization effects). Only two parameters, the subcell edge c_s along the chain axis and the positional parameter x of the center of one molecule, were varied in a least-squares analysis. The setting angle was set equal to 41·3°, as derived from birefringence measurements. Best agreement between observed and calculated intensities was obtained for $c_s = 2{\cdot}5454$ and the value x given in Table 1 which gives the fractional coordinates of the centres of the four paraffin chains in a unit cell.

Table 1. $C_{33}H_{68}$, *modification A: fractional coordinates of the centres of the four paraffin molecules* M_1, M_2, M_3, M_4 *contained in the unit cell*

	x	y	z
M_1	0·078	0·25	0·25
M_2	0·922	0·75	0·75
M_3	0·578	0·75	0·25
M_4	0·422	0·25	0·75

Figs. 6 and 7 show schematically the chain packing in modification *A*. The subcell is orthorhombic with edges

$$a_s (= a) = 7{\cdot}44 \pm 0{\cdot}005 \text{ Å}$$
$$b_s (= b) = 4{\cdot}96 \pm 0{\cdot}005$$
$$c_s = 2{\cdot}5454 \pm 0{\cdot}001$$

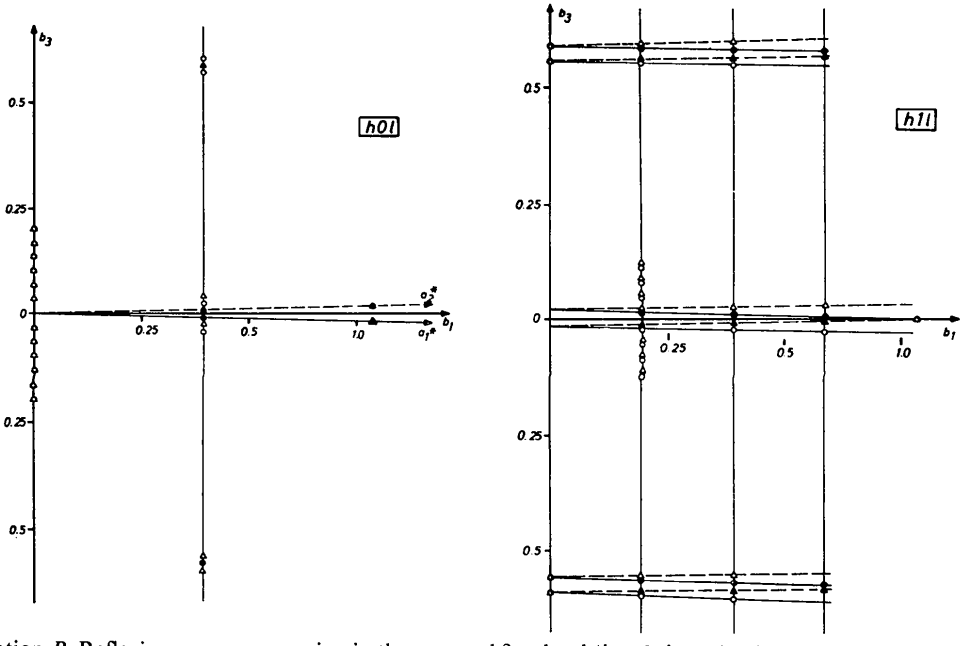

Fig. 8. Modification *B*. Reflexion groups appearing in the zero and first level ($b_2 = 0$, $b_2 = 1/4{\cdot}98$) upon rotation of the crystal about x_2. The crystal is twinned. Reflexions of the two components are distinguished by circles and triangles. The two individuals differ in the directions $\mathbf{a}_1^*$, $\mathbf{a}_2^*$ of their reciprocal lattice.

and contains two methylene groups. Stacking parameters are:

$$\Delta_{ch}(=c/2)=43{\cdot}8\ \text{Å}$$
$$\Delta_a=\pm 0{\cdot}156\times a=1{\cdot}16\ \text{Å}$$
$$\Delta_b=\pm b/2=2{\cdot}48\ \text{Å}$$

where Δ_a and Δ_b describe the shift parallel to **a** and **b** respectively. These shifts occur in opposite directions for successive pairs of layers. The translation is accompanied by a 180° turn about the chain direction.

2. *Modification B* ($54{\cdot}5\,°C < T < 65{\cdot}5\,°C$)

The phase transition $A \rightarrow B$ leaves the external appearance of the crystals unchanged, but alters the diffraction pattern.

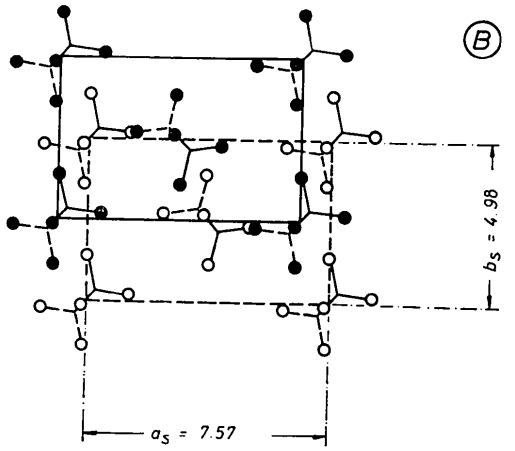

Fig. 9. Modification *B*. Packing of chains in two successive lamellae. Projection along the chain axis.

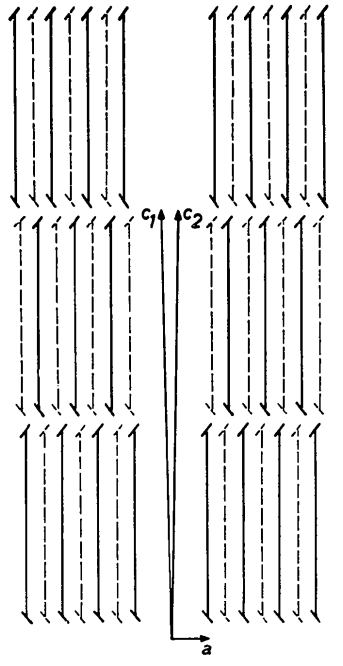

Fig. 10. Modification *B*. Projection along x_2. Schematic drawing of the packing of chains in the two components of the twinned crystal.

From oscillation photographs a monoclinic axis parallel to x_2 was located with a cell length of 4·98 Å. The reflexion positions in the zero and first level were mapped by Weissenberg photography and are shown in Fig. 8. Reflexion groups appear localized at the same positions as for modification *A*, the splitting direction being unchanged. Only the spacings within the reflexion groups are altered.

These findings permit the following conclusions. The subcell remains orthorhombic, its orientation being preserved. Furthermore, the lamellar surfaces continue to be oriented with their normal parallel to the chain direction. The centres of the reflexion groups yield the edge lengths of the subcell. At 60 °C, the temperature of the measurement, they are

$$a_s=7{\cdot}567\pm 0{\cdot}005\ \text{Å}$$
$$b_s=4{\cdot}976\pm 0{\cdot}005$$
$$c_s=2{\cdot}545\pm 0{\cdot}015\ .$$

The positions of the 00*l* reflexions correspond to a lamellar thickness $L=43{\cdot}96$ Å. The observed non-equidistant spacings of the reflexions in a group suggest that the crystal is twinned, which is confirmed by a detailed analysis. The crystal consists of components with two different structures. Their reflexions are distinguished in Fig. 8 by circles and triangles. The two types differ in the layer stacking, the single layers being identical. The stacking parameters can be derived directly from the geometrical data. They are

$$\Delta_{ch}=L=43{\cdot}96\ \text{Å}$$
$$\Delta_b=b_s/2=2{\cdot}49\ \text{Å}$$
$$\Delta_a=0{\cdot}125\times a_s=0{\cdot}95\ \text{Å, for one type,}$$

and

$$\Delta_{ch}=L=43{\cdot}96\ \text{Å}$$
$$\Delta_b=b_s/2=2{\cdot}49\ \text{Å}$$
$$\Delta_a=-0{\cdot}125\times a_s=-0{\cdot}95\ \text{Å for the other.}$$

The layers are stacked without any rotation of the lamellae by constant translations specified by Δ_a, Δ_b, Δ_{ch}. The packing which results is represented schematically in Fig. 9. The two structures are related by a reflexion at the lamellar surface, which may be considered as a twinning plane common to adjacent individuals of different type.

The two unit cells can be chosen with common edges *a*, *b* and with the *c* axes inclined in different directions (Fig. 10). The inclination angle to the chain direction is directly related to the stacking parameter Δ_a. Both values follow from the reflexion positions (compare Fig. 8). The resulting unit cell is monoclinic with lattice constants

$$a(=a_s)=7{\cdot}57\pm 0{\cdot}005\ \text{Å}$$
$$b(=b_s)=4{\cdot}98\pm 0{\cdot}005$$
$$c(=2L/\sin\beta)=87{\cdot}94\pm 0{\cdot}02$$
$$\beta=91{\cdot}2\text{ or }88{\cdot}8°.$$

The space group is *Aa* [the (100)-lattice plane is centred]. The unit cell contains four molecules. As required by the space group *Aa*, reflexions are limited by the conditions hkl: $k+l=2n$; $h0l$: $h=2n$.

Corresponding reflexions of the two types of components are of equal intensity. Hence both share equal parts in the crystal. The scattering pattern as a whole preserves its original orthorhombic symmetry.

We stress that the stacking parameters of modification *B* followed solely from the reflexion positions. In contrast to the analysis of the scattering pattern of modification *A*, no structure-factor calculations were necessary for a characterization of the layer stacking.

The setting angle φ, estimated from birefringence measurements, is 42·5°.

3. *Modification C* (65·5 °C < *T* < 68 °C)

The phase transition $B \rightarrow C$ is accompanied by a clearly visible change in the surface structure of the crystals. Fine, regular striations appear parallel to $\mathbf{x}_2$ (Fig. 11). Oscillation photographs show a monoclinic axis in this direction with a length of 4·98 Å. Zero and first-level Weissenberg photographs were taken in order to map the distribution of reflexions (Fig. 12).

The following conclusions may be drawn. The general positions of the reflexion groups remain unchanged after the transition. Hence, the subcell is orthorhombic as for modifications *A* and *B* and its orientation is largely kept constant. Two distinct splitting lines with different orientations appear for each subcell reflexion. This indicates the presence of two types of lamellar surfaces, the normals being perpendicular to x_2 and enclosing angles of $\pm 16{\cdot}5°$ with x_3. Thus the crystal is again twinned. The observed striations reflect ridges in the original plane surface. The reciprocal lattices of the two type of individual components have common edges in the directions $\mathbf{b}_1$ and $\mathbf{b}_2$. Hence, both have a common direct axis parallel to x_3, and the unit cells can be chosen as indicated in Fig. 13. The cells are monoclinic with lengths (at 66 °C):

$$a = 8{\cdot}02 \pm 0{\cdot}005 \text{ Å}$$
$$b = 4{\cdot}985 \pm 0{\cdot}005$$
$$c = 88{\cdot}0 \pm 0{\cdot}2 .$$

The monoclinic angle is $\beta = 106{\cdot}5$ or $73{\cdot}5°$.

After separating and indexing the reflexions (again circles and triangles are used to distinguish between the two series in Fig. 12) one limiting condition is found: hkl: $k+l=2n$. This permits three possible space groups: *Am*, *A*2/*m*, *A*2. The only one which is compatible with an orthorhombic subcell having no mirror plane perpendicular to $\mathbf{b}_s$ is *A*2.

Next we need to know the exact chain direction, which might deviate slightly from the *c* axis. For this purpose powder patterns were recorded with a diffractometer for an estimation of the intensities of the reflexions groups around the subcell reflexions 200_s, 110_s. The observed intensities were compared with values calculated for different inclination angles ε between the chain axis and the cell edge *c*. This restricted structure-factor calculation led to the conclusion that ε should lie in the range $\varepsilon = 2 \pm 0{\cdot}3°$, with a tilting direction as indicated in Fig. 13. As a result, the angle enclosed by the chain axis and the normal to the lamellar surface is $18{\cdot}5 \pm 0{\cdot}3°$. The most probable value is 18·5°, since for this value the lamellar surfaces correspond to $(101)_s$ and $(10\bar{1})_s$ planes of the subcell lattice. This means that the oblique lamellae found for modification *C* emerge from the rectangular lamella of modifications *A* and *B*

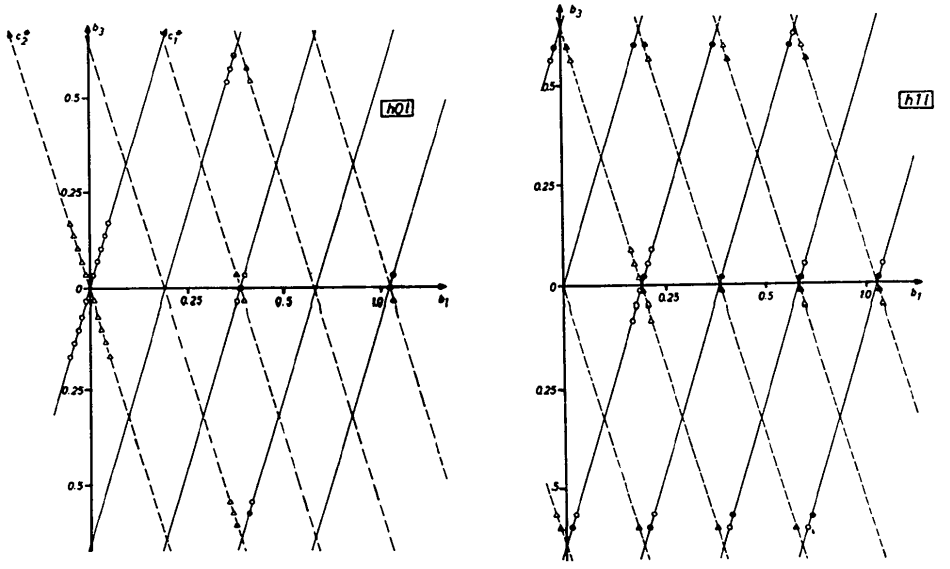

Fig. 12. Modification *C*. Reflexion groups appearing in the zero and first level ($b_2=0$, $b_2=1/4{\cdot}985$) upon rotation of the crystal about x_2. The crystal is twinned. The two individuals differ in the directions $\mathbf{c}_1^*$, $\mathbf{c}_2^*$ of their reciprocal lattices. They are distinguished by circles and triangles. The strongest reflexion in each group is marked by a filled circle or triangle.

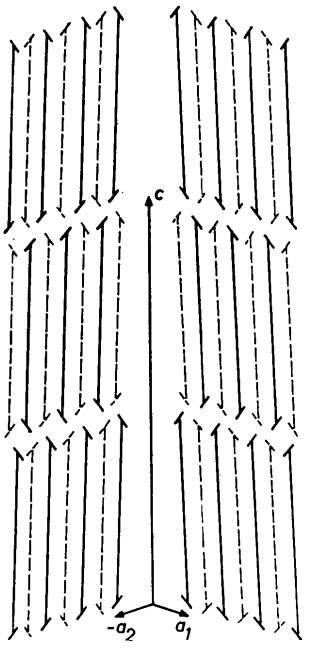

Fig. 13. $C_{33}H_{68}$. Appearance of a crystal during the phase-transition $B \rightarrow C$.

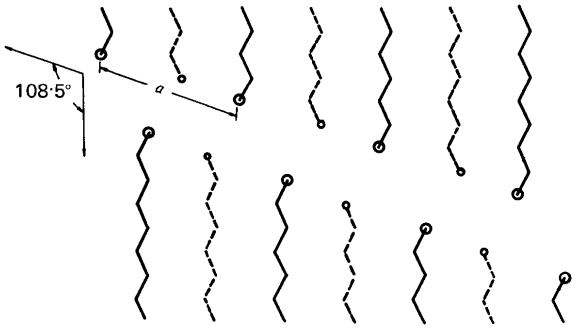

Fig. 14. Modification *C*. Schematic drawing of the packing of chains in the two components of the twinned crystal in projection along x_2.

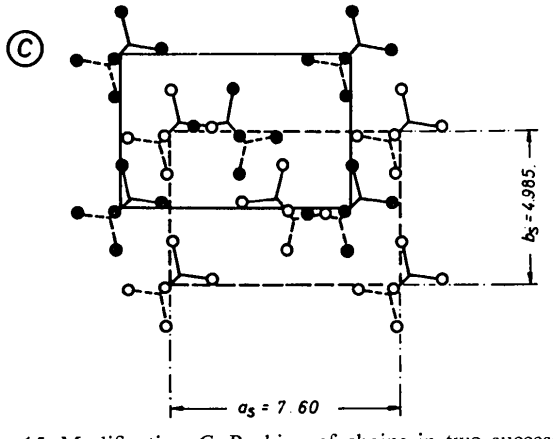

Fig. 15. Modification *C*. Packing of chains in two successive lamellae. Projection along the chain axis.

by a relative shift of $c_s = 2{\cdot}54$ Å between neighbouring (100) lattice planes. The resulting surface structure and the packing of neighboring surfaces is shown in Fig. 14. Fig. 15 shows the chain packing in projection along the chain axis. The subcell is orthorhombic, with (at 66 °C):

$$a_s(=a\times\cos 18{\cdot}5°) = 7{\cdot}60 \pm 0{\cdot}005 \text{ Å}$$
$$b_s(=b) = 4{\cdot}985 \pm 0{\cdot}005$$
$$c_s = 2{\cdot}545 \pm 0{\cdot}015$$

Stacking occurs by constant translations. The stacking parameters are

$$\Delta_{ch}(=\tfrac{1}{2}c\times\cos 16{\cdot}5°/\cos 18{\cdot}5°) = 44{\cdot}5 \text{ Å}$$
$$\Delta_b = 0{\cdot}5\times b = 2{\cdot}49 \text{ Å}$$

and

$$\Delta_a = 0{\cdot}2\times a = 1{\cdot}62 \text{ Å, for one type,}$$
$$\Delta_a = -1{\cdot}62 \text{ Å for the other.}$$

Owing to the fine striations, optical determination of the setting angle φ was impossible. It will probably not differ significantly from the one measured at the end of modification *B*, *i.e.* $\varphi \approx 42{\cdot}5°$.

By comparison of the intensities we found that both types of individuals contribute equally to the twin. Thus the crystal as a whole preserves its original symmetry.

Owing to the staggering of chains the lamellar thickness *L*, measured perpendicular to the lamellar surface, is smaller than in the preceding modifications. It is $L = \frac{1}{2}c\times\cos 16{\cdot}5° = \Delta_{ch}\cos 18{\cdot}5° = 42{\cdot}2$ Å.

4. *Modification D* (68 °C < *T* < 71·8 °C)

Observations in the polarizing microscope show that the transition to modification *D* occurs in two successive steps. At first the striations characteristic of modification *C* disappear completely and the crystal recovers its plane surface. No birefringence can be observed; the optical axis is perpendicular to the lamellar surface. This is a transition state and is stable only within an extremely narrow temperature range of the order of 0·1 °C. Subsequently coarse wrinkles develop on the surface roughly parallel to the short diagonal or to the lozenge edges (Fig. 16). This last phase, modification *D*, exists up to the melting point $T_m = 71{\cdot}8$ °C.

Powder diagrams were recorded with the diffractometer. The 00*l* reflexions are sharp and yield a lamellar thickness $L = 42 \pm 0{\cdot}1$ Å. Three strong reflexions and two very weak ones appear in the scattering range $20° < 2\theta < 25°$, where the low-order lateral reflexions lie. They have positions corresponding to interplanar spacings $d = 4{\cdot}235 \pm 0{\cdot}005$; $4{\cdot}115 \pm 0{\cdot}005$; $4{\cdot}065 \pm 0{\cdot}005$; $4{\cdot}00 \pm 0{\cdot}01$; $3{\cdot}93 \pm 0{\cdot}01$ Å, and are superimposed on a halo (Fig. 17). Higher orders have extremely low intensities. We could detect only one other halo in the scattering range of the subcell reflexions $h11_s$, $h = 0, \pm 1, \pm 2$ (referred to the orthorhombic subcell, Fig.

2), and two broad reflexions probably corresponding to 310_s and 020_s.

This scattering behaviour is typical for a highly disordered crystalline lattice. The lateral order and the layer stacking are clearly strongly disturbed.

Oscillation photographs showed that a crystallographic axis is parallel to x_2. Zero and first-level Weissenberg photographs were taken. The reflexion positions found are given in Fig. 18. Owing to the poor quality of the Weissenberg photographs, an exact determination of the positions of the lateral reflexions was impossible. They are represented in Fig. 18 by spheres with volumes corresponding to the uncertainty involved. Each of the three pairs of lateral reflexions appears at 6 different positions. The reflexions lie on straight lines along $\mathbf{b}_3$, starting from the corners of a regular hexagon with an edge of reciprocal length $|b|=0{\cdot}2345$ Å^{-1}. There are indications that the reflexions are not strictly collinear. These possible systematic deviations are certainly smaller than the radius of the plotted spheres and will not influence our main conclusions. In contrast to the lateral reflexions the $00l$ reflexions take unique positions along the b_3 axis.

The multiple-reflexion positions indicate that the crystal is a multiple twin. The observed relative intensities vary greatly for different samples, which indicates variations in their composition. This property enabled us to analyse the correlations in the intensities in order to identify the sets of related reflexions stemming from the different individuals. One set is plotted in Fig. 18, by filled circles (this set actually represents the result of one experiment where accidentally only one individual was in the beam). The different individual components transform by 60° turns about the x_3 axis, or by reflexion at the planes perpendicular to the axes x_1, x_2, x_3.

These findings allow the following conclusions. The chain axis which runs perpendicular to the plane common to the six main lateral reflexions is tilted with respect to the normal to the lamellar surface; thus we have oblique layers. The individual parts differ in their chain direction. Tilting occurs alternatively parallel to the lozenge edges or to the short diagonal. The layer surface is oriented perpendicular to x_3 for all individuals.

The three pairs of lateral reflexions show different reflexion angles. This indicates that the unit cell is triclinic. Nevertheless the symmetry of the sublattice could be orthorhombic with two pairs of subcell reflexions (110_s, $\bar{1}\bar{1}0_s$; $\bar{1}10_s$, $1\bar{1}0_s$) corresponding to $d\simeq 4{\cdot}09$ Å, and one pair (200_s, $\bar{2}00_s$) to $d\simeq 4{\cdot}23$. Stacking can cause a shift in the observed values. However, this remains a speculation, and one cannot exclude the possibility that the subcell is triclinic with only one methylene group per subcell. The critical reflexion 210_s which can distinguish between these two types (it vanishes on passing from the orthorhombic to the triclinic subcell) was not observable. In any case the lateral packing is not hexagonal. Assuming an

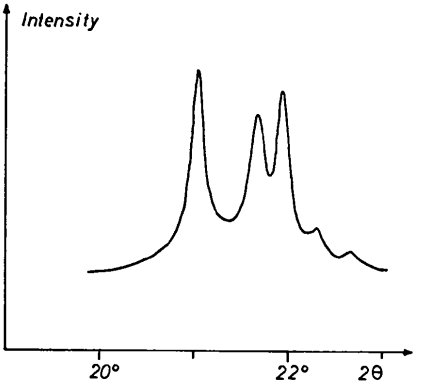

Fig. 17. Modification *D*. Diffractometer curve showing three strong lateral reflexions.

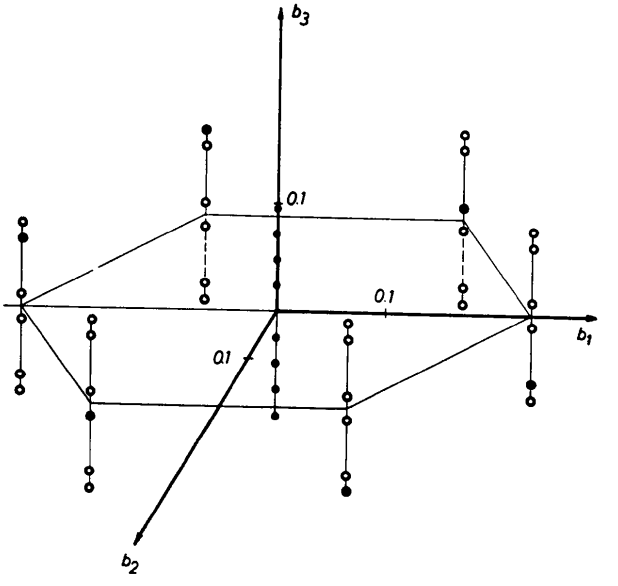

Fig. 18. Modification *D*. Positions of the three pairs of lateral reflexions (shown in Fig. 17) in reciprocal space. The crystal is a multiple twin. A set of related reflexions stemming from one component is plotted as filled circles.

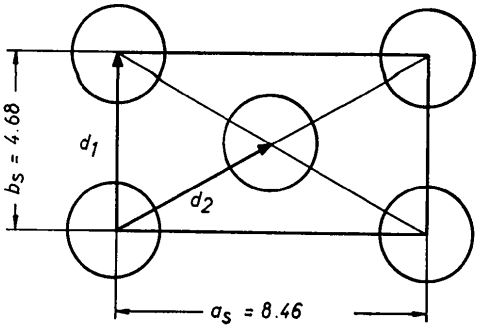

Fig. 19. Modification *D*. Lateral packing of chains assuming an orthorhombic subcell. Chain cross sections are plotted as circles.

orthorhombic subcell two different distances between the axes of neighbouring chains follow, taking the values $d_1 \simeq 4{\cdot}68$ and $d_2 \simeq 4{\cdot}83$ Å. Fig. 19 shows a schematic diagram with the chains represented by circles. Each chain occupies an area $S = 19{\cdot}8$ Å^2.

The reflexion positions change slightly with increasing temperature. The values given above were measured at 69 °C. At 71 °C the three characteristic lateral reflexions are found at positions corresponding to $d =$ 4·215, 4·13, 4·08 Å. Thus hexagonal symmetry is further approached but not reached.

The reflexion positions provide an estimate for the inclination angle of the chain axis to the surface normal. The six strong lateral reflexions plotted with filled circles in Fig. 18 are coplanar within the error of measurement. The normal to this plane, which gives the chain direction, encloses an angle of 19·5° with the surface normal. Strictly speaking, we should use the unknown exact positions of the subcell reflexions, which may lie at slightly shifted points; furthermore, the positions of the observed reflexions are somewhat uncertain. Therefore the inclination angle given has a possible error of $\pm 2°$.

A lamellar surface with this orientation does not represent a simple lattice plane in a sublattice with cell dimensions $a_s = 8{\cdot}46$, $b_s = 4{\cdot}68$ Å, as indicated in Fig. 19, and $c_s = 2{\cdot}54$ Å. From the observed direction of tilt one concludes that it should be a $(0kl)_s$ plane. A planar array of the end groups is achieved only for the series $(0k1)_s$, $k = 0, \pm 1, \pm 2, \ldots$. The normal to the lattice-plane $(011)_s$, which yields the lowest inclination angle, encloses an angle of 28·5° (= arctan 2·54/4·68) with the chain direction $\mathbf{c}_s$. This is definitely larger than the measured one. Hence, staggering of neighbouring $(010)_s$ planes occurs with irregular shifts with an average of $2 \times 2{\cdot}54$ over 3 neighbouring lattice planes (tan $19{\cdot}5° = 2 \times 2{\cdot}54/3 \times 4{\cdot}68$).

The layer stacking seems to be partly regular, partly irregular, probably due to stacking faults. Only a regular stacking can cause the observed reflexions, which show widths only slightly broader than for the preceding modifications. On the other hand, stacking faults may contribute to the observed halo. A more detailed derivation of the layer stacking seems difficult. As a consequence no crystallographic unit cell is specified.

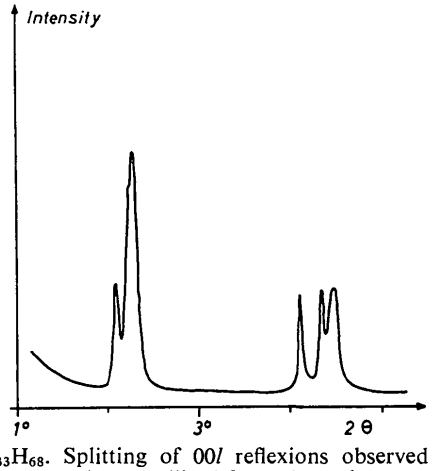

Fig. 20. $C_{33}H_{68}$. Splitting of 00l reflexions observed with a sample crystallized from the melt.

Observations during the cooling process

When a crystal is cooled from the temperature range of modification D, transition to C occurs with slight ($\simeq 1$ °C) undercooling. With the transition the wrinkles on the surface partly disappear. The crystal looks as if it were divided into sections of approximately triangular shape, the triangle edges being roughly parallel to the short diagonal and the edges of the lozenge. Optical measurements indicate, and X-ray scattering experiments confirm, that each section represents an individual part with characteristic chain direction, the chain packing being the same as in C. Thus, in contrast to its structure in phase C during the initial heating, the crystal is now built up of six types of individuals with different chain directions but common orientation of the lamellar surfaces. The typical ridges observed during heating for modification C (Fig. 11) do not reappear.

The high-temperature modifications C, D can be partly frozen and observed at room temperature. This shows up most directly in the lamellar reflexions 00l, which appear to be due to the superposition of several components after cooling samples from the melt, or from phase D. Fig. 20 shows a typical example. The two superposed series with sharp reflexions yield values $L = 43{\cdot}8$ and 41·7 Å and represent modification A and the supercooled modification C. The third series, showing very broad reflexions, corresponds to values lying around $L = 40$ Å. It probably represents a state of order developed from modification D, as for example oblique lamellae with surfaces roughly parallel to $(011)_s$ planes. These metastable states can be largely removed by annealing samples at temperatures around 60 °C.

Discussion

Two minor differences are noted when comparing the structure of modification A with that given by Smith (1953) for $C_{23}H_{48}$. First we found smaller lattice constants ($a = 7{\cdot}44$, $b = 4{\cdot}96$ *versus* $a = 7{\cdot}48$, $b =$ 4·97 Å). This is in accordance with a general tendency observed for the homologous series of n-alkanes where the cross-sectional area per chain decreases with increasing chain length (Vand & de Boer, 1947). Secondly, Smith specifies the setting angle only very roughly as $\varphi = 48 \pm 5°$. This considerable error range reflects the difficulty of deriving a reliable value from X-ray experiments alone. In our opinion a better estimate follows from the measured birefringence, which yielded $\varphi = 41{\cdot}3°$ (since $n_b > n_a$ we certainly have $\varphi < 45°$). The difference in the values measured for c ($C_{33}H_{68}$: 87·7 Å; $C_{23}H_{48}$: 62·3 Å) corresponds to the

different chain lengths of the compounds (25·4 Å = $2 \times 10 \times 1{\cdot}27$ Å).

So far no structure similar to modification *B* has been reported. One would expect to find this structure generally with odd-numbered paraffins of comparable chain length. The occurrence of an observable sharp phase transition is certainly very sensitive to the purity.

Modification *C* could be similar to or even identical with a phase of a yet unknown structure which has been reported to exist for $C_{36}H_{74}$ in a small temperature range immediately below the rotational transition (Schaerer, Busso, Smith & Skinner, 1955). Upon heating this compound Keller (1961) observed striations running parallel to the diagonals of the crystals. His suggestion that the striations reflect ridges on the surface has been confirmed by our results.

The chain packing in the so-called rotator phase, our modification *D*, is definitely different in $C_{33}H_{68}$ from that given by Larsson (1967) for $C_{19}H_{40}$. Our findings, which indicate deviations from hexagonal packing and tilting of the chains, suggest that the popular simple rotator-model is too limited, since it requires strict hexagonal symmetry for the lateral packing and cannot explain the chain tilting. It is possible that the observed transition state with vanishing birefringence corresponds to Larsson's structure.

Preliminary measurements on samples of $C_{34}H_{70}$ and $C_{36}H_{74}$ indicate that modification *D* is not a peculiarity of the odd-numbered paraffin $C_{33}H_{68}$ but is the chain packing in the 'rotator-phase' for all paraffins, even and odd numbered, with comparable chain length. We found the lamellar thickness in this phase to be $L = 43{\cdot}2 \pm 0{\cdot}5$ for $C_{34}H_{70}$ and $L = 45{\cdot}5 \pm 0{\cdot}5$ Å for $C_{36}H_{74}$, which indicates tilting of the chains with an angle of about 19° to the surface normal.

The structures of modifications *B*, *C* and *D* cannot be understood from static packing considerations without taking into account the dynamics of the chains. The observed phase transitions can be regarded as reactions of the crystal lattice to the onset of certain chain motions which bring disorder into the crystal. Chain rotation is the only mechanism discussed so far. Our results suggest that not one but several distinguishable types of chain motion can be active. In forthcoming papers (Strobl, Ewen, Fischer & Piesczek, 1974) we shall report the results of small-angle X-ray scattering experiments, for examining defect structures in the lamellar interfaces, and of n.m.r. and infrared measurements performed in order to investigate molecular motion. A joint discussion of all structural and dynamical properties observed with crystals of $C_{33}H_{68}$ will be given in these papers.

A prerequisite for this work was the synthesis of pure tritriacontane. We are grateful to Professor W. Heitz and Dr R. Peters for their cooperation. Thanks are due to Professor E. W. Fischer for his continuous support in numerous helpful discussions. This research was supported by the Deutsche Forschungsgemeinschaft (Sonderforschungsbereich 41).

References

BROADHURST, M. (1962). *J. Res. Natl. Bur. Stand.* **66**, 241–249.

HARTSHORNE, N. H. & STUART, A. (1970). *Crystals and the Polarizing Microscope*, p. 156. London: Arnold.

HEITZ, W., WIRTH, T., PETERS, R., STROBL, G. & FISCHER, E. W. (1972). *Makromol. Chem.* **162**, 63–79.

HOFFMANN, J. D. (1952). *J. Chem. Phys.* **20**, 541–549.

KELLER, A. (1961). *Phil. Mag.* **63**, 329–339.

KITAIGORODSKII, A. (1961). *Organic Chemical Crystallography*, pp. 177–208. New York: Consultants Bureau.

LARSSON, K. (1967). *Nature, Lond.* **213**, 383–384.

MCCLURE, D. (1968). *J. Chem. Phys.* **49**, 1830–1839.

MÜLLER, A. (1932). *Proc. Roy. Soc.* A **138**, 514–540.

MÜLLER, A. & LONSDALE, K. (1948). *Acta Cryst.* **1**, 129–131.

SCHAERER, A. A., BUSSO, C. J., SMITH, A. E. & SKINNER, L. B. (1955). *J. Amer. Chem. Soc.* **77**, 2017–2019.

SEGERMAN, E. (1965). *Acta Cryst.* **19**, 789–796.

SHEARER, H. M. M. & VAND, V. (1956). *Acta Cryst.* **9**, 379–384.

SMITH, A. E. (1953). *J. Chem. Phys.* **21**, 2229–2231.

STROBL, G., EWEN, B., FISCHER, E. W. & PIESCZEK, W. (1974). Submitted for publication in *J. Chem. Phys.*

VAND, V. & DE BOER, R. (1947). *Proc. Koninkl. Ned. Akad. Wetenschap.* **50**, 991–999.